MODELLISTICA E CALCOLO SCIENTIFICO

MODELING AND SCIENTIFIC COMPUTING

MOX–Report No. 11/2009

Implicit tracking for multi-fluid simulations

Luca Formaggia, Andrea Villa

MOX, Dipartimento di Matematica "F. Brioschi"
Politecnico di Milano, Via Bonardi 9 - 20133 Milano (Italy)

mox@mate.polimi.it http://mox.polimi.it

Implicit tracking for multi-fluid simulations. *

L. Formaggia ♯, A. Villa ‡

April 6, 2009

♯ MOX– Modellistica e Calcolo Scientifico
Dipartimento di Matematica "F. Brioschi"
Politecnico di Milano
via Bonardi 9, 20133 Milano, Italy
mox@mate.polimi.it

‡ Dipartimento di Matematica "F. Eriquez"
Universita' degli studi di Milano
via Saldini 50, 20133 Milano, Italy
andrea.villa@unimi.it

Keywords: level set, volume of fluid, multi-fluid simulations

AMS Subject Classification: 35L45, 35L65

Abstract

In this work a new coupled level set - volume tracking method is introduced. To advance the solution in time, a MUSCL-type method combined to a new flux limiter is used. It is shown that our discrete method has many interesting properties that make it suitable for problems where the tracking of a large number of regions is needed. A dedicated reconstruction algorithm for the level set reinizialization is also provided. We show some numerical tests demonstrating its effectiveness for multi-fluid problems.

1 Introduction

In this paper we illustrate a method to track separating interfaces among immiscible fluids when a large number of fluids is involved. We consider only a passive advection i.e. the velocity field is a given quantity. Our aim is to construct a robust method, effective even when the interfaces experience deformations, with good mass conservation properties and that can be used on (2D and 3D) unstructured meshes.

*This work has been supported by the Project: Steam3D - ENI

In the literature many techniques regarding the two fluid problem are reported but often they cannot be extended readily to the multi-fluid problem and, moreover, do not match all of our requirements. Tracking methods can be subdivided into two categories: the Lagrangian and the Eulerian ones. The former track the interfaces explicitly, while the latter reconstruct them with a post-processing procedure. Among the many Lagrangian tracking algorithms (see, for instance, [14], [28], [20]), some move all the volume mesh nodes, some others track only the interface points and reconstruct the mesh in the interior at every time step, or whenever necessary. The Lagrangian approach presents many difficulties, particularly in three-dimensional computations, such as the treatment of possible topological changes. Furthermore, sophisticated adaption algorithms should be used to guarantee a sufficient mesh quality. The tracking of surfaces only has less severe regularity issues since fewer nodes have to be moved. However, in the cases where the fluid velocity is not given but has to be computed, we usually have to solve a differential problem on a fixed grid. And we need to know, in every point of the computational domain, which of the fluids is present. This implies an interpolation procedure for the data at the interface between fluids. These interpolation techniques add computational burden and introduce numerical errors. Although the notable advances in efficient techniques for automatic topology indentification and reconstruction developed in [6], yet these methods are not mature enough to be implemented in a general multi-fluid code. In many cases the Lagrangian approach could be computationally cost effective only if no topological change occurs. Otherwise, complex topology correction algorithms are needed (see, for instance, the one in [16]). Furthermore, it's often impossible to prove the algorithm robustness with respect to topological changes in complex and realistic 3D situations. Though the Lagrangian methods have an explicit and immediate representation of the interfaces (see [14], [20], [12], [28]) they are not conservative. Some works, for example [27], [23], have been proposed to solve the topological change problem. These approaches require a fixed background grid for the solution of a geometry regularization equation. Though interesting, they apply only to two fluid simulations and are not mass-preserving. There are works, like [15], which present procedures to enforce mass conservation, but fail to be robust for topological changes.

The complexity of Lagrangian methods triggered the development of the Eulerian implicit tracking methods: an overview of these can be found in [11] and [7]. We remind the properties of the most effective ones, namely the volume of fluid (VOF) and the level-set (LS) method. Other, mixed Eulerian-Lagrangian, methods exist, such as the ALE methods [9] or the particle methods [17], but none of them have the characteristics we are looking for. The LS [10], [24] is a robust method and is easy to code, but in its usual form does not fit the multi fluid framework and, in many cases, does not conserve mass. Indeed, the distance function, normally used as the tracking function, fails to guarantee a coherent reconstruction of the interfaces when more than two fluid species are involved. Many works are devoted to fix the LS drawbacks, like [26] and [19],

yet all of them consider only the case of two fluids. The mass conservation issue can be partially solved by refining the grid adaptively, as pointed out in [1] and [2]. VOF methods are mass conservative by construction and relatively robust although they are usually designed to track only two fluids and moreover they have, in general, an irregular reconstruction of interfaces. The principal difficulty is again the non-coherence between the reconstruction of the interfaces when more than two fluids are involved. Interface reconstruction using the VOF methods is a major topic and many works such as [3], [4] are devoted to it. However the multi-fluid case is not usually treated and many VOF algorithms require a structured mesh. One of the most applicable methods for multi-fluid simulations is the partial volume tracking method (VT) (see [11] for a brief description) which consists in discretizing with high order schemes the volume transport equation. This approach has a moderate success, yet the discontinuous initial solutions are quickly diffused even if high resolution methods are used.
In the first part of this paper we present a VT and LS coupling that combines the best features of both the schemes, moreover we introduce a flux-limited of MUSCL type scheme (see [5] for MUSCL schemes and [13] about the limiter theory) which is capable to work on unstructured meshes and has a low numerical diffusion. In the second part we analyze the properties of our method and finally we show its numerical performances.

2 The method

We consider a domain $\Omega \subset \mathbb{R}^d$ with regular boundary $\partial\Omega$; this domain is filled with n_s immiscible fluid species, such that every subdomain $\omega_i \subset \Omega$, corresponding to a species, does not overlap with the others and $\overline{\Omega} = \bigcup_{i=0}^{n_s} \overline{\omega}_i$. The subdomains ω_i depend on time, i.e. $\omega_i = \omega_i(t)$, since they are advected by a time dependent velocity field $\overrightarrow{V}(t, \overrightarrow{X})$, $\overrightarrow{X} \in \Omega$ and $t \geq 0$, whose trace on $\partial\Omega$ has zero normal component, i.e. $\overrightarrow{V} \cdot \overrightarrow{n} = 0$ on $\partial\Omega$, being $\overrightarrow{n}$ the boundary normal versor. We define $\lambda_i^0 \in L^2(\Omega)$ as the characteristic function of the subdomain ω_i at initial time, i.e. $\lambda_i^0(\overrightarrow{X}) = \chi_{\omega_i(0)}$ where:

$$\chi_{\omega_i(t)}(\overrightarrow{X}) = \begin{cases} 1, & \text{if } \overrightarrow{X} \in \omega_i(t) \\ 0, & \text{if } \overrightarrow{X} \notin \omega_i(t) \end{cases}$$

for $i = 0, \ldots, n_s$. Therefore the following relation holds: $\sum_{i=1}^{n_s} \lambda_i^0 = 1$ almost everywhere in Ω. Let's introduce the VT equation for a given vector field $\overrightarrow{V}$:

$$\begin{cases} \dfrac{\partial \lambda_i}{\partial t} + \overrightarrow{\nabla} \cdot (\lambda_i \overrightarrow{V}) - \lambda_i (\overrightarrow{\nabla} \cdot \overrightarrow{V}) = 0 \quad t > 0, \quad i = 1, \ldots, n_s \\ \lambda_i = \lambda_i^0; \quad t = 0 \end{cases} \tag{1}$$

where $\lambda_i(t, \cdot) \in L^2_\Omega$ is a weak solution of (1). This equation is equivalent to the

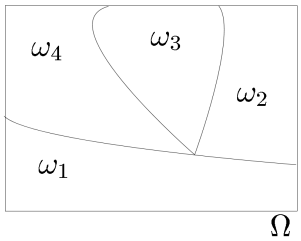

Figure 1: Domain Ω and its subdomains ω_i.

transport equation:

$$\frac{\partial \lambda_i}{\partial t} + \overrightarrow{V} \cdot \overrightarrow{\nabla} \lambda_i = 0 \tag{2}$$

and we account for non-solenoidal velocity fields. Problem (1) has some properties we wish to recall.

Proposition 2.1 *If the initial condition satisfies* $\sum_{i=1}^{n_s} \lambda_i^0 = 1$ *almost everywhere in* Ω *then* $\sum_{i=1}^{n_s} \lambda_i = 1, \forall t > 0$ *almost everywhere in* Ω.

Proof: Summing up the i-th equations in (1) we get:

$$\frac{\partial}{\partial t}\left(\sum_{i=1}^{n_s} \lambda_i\right) + \overrightarrow{\nabla} \cdot \left(\overrightarrow{V} \sum_{i=1}^{n_s} \lambda_i\right) - (\overrightarrow{\nabla} \cdot \overrightarrow{V}) \sum_{i=1}^{n_s} \lambda_i = 0 \tag{3}$$

We state that $\sum_{i=1}^{n_s} \lambda_i = 1, \forall t \geq 0$ is a solution of (3) and it satisfies the initial condition. From the linearity of the problem it follows that the solution is also unique. ■

Proposition 2.2 *If the initial condition satisfies* $0 \leq \lambda_i^0 \leq 1$ *almost everywhere in* Ω *and the velocity field* $\overrightarrow{V}$ *is bounded and Lipschitz continuous with respect to the space variables, uniformly in* t*, then* $0 \leq \lambda_i \leq 1, \forall t > 0$ *almost everywhere in* Ω.

Proof: We use a standard characteristic theory argument. Equation (2) written in the characteristic metric reads:

$$\frac{d}{dt}\lambda_i(t, \overrightarrow{P}(t)) = 0 \text{ almost everywhere in } \Omega$$

where $\overrightarrow{P}(t, \overrightarrow{X})$ is the characteristic metric. Therefore for almost all $\overrightarrow{X}$ there exists a $\overrightarrow{P}(0, \overrightarrow{X})$ such that $\lambda_i(t, \overrightarrow{X}) = \lambda_i(t, \overrightarrow{P}(0))$ and the thesis follows. ■
Let's pass to the level set definition, we define $\phi_i : \mathbb{R}^+ \times \overline{\Omega} \to \mathbb{R}$, with $\phi_i(t, \cdot) \in \mathbb{C}^0(\overline{\Omega}) \quad \forall t > 0$, $i = 1, \ldots, n_s$, some level set functions such that $\omega_i(t) = \{\overrightarrow{X} \in$

$\overline{\Omega} : \phi_i(t, \overrightarrow{X}) > \frac{1}{2}\}$ and consequently $\partial\omega_i(t) = \{\overrightarrow{X} \in \overline{\Omega} : \phi_i(t, \overrightarrow{X}) = \frac{1}{2}\}$. This particular value of the set will be useful when we find an analogy between the discrete forms of LS and the VT equations. We can write the following evolution equation for each ϕ_i:

$$\begin{cases} \dfrac{\partial \phi_i}{\partial t} + \overrightarrow{\nabla} \cdot (\phi_i \overrightarrow{V}) - \phi_i(\overrightarrow{\nabla} \cdot \overrightarrow{V}) = 0; \quad t > 0 \\ \phi_i = \phi_i^0; \quad t = 0 \end{cases} \tag{4}$$

by which at all times $\lambda_i = H\left(\phi_i - \frac{1}{2}\right)$, where:

$$H(\varrho) = \begin{cases} 1 \text{ if } \varrho > 0 \\ 0 \text{ otherwise} \end{cases}$$

is the Heaviside function, and ϕ_i^0 is the initial condition. In other words, at the continuous level, equations (1) and (4) are two equivalent ways to describe the interface motion. However, in the discrete setting we will use two different spaces for the discrete λ_i and ϕ_i, leading to a new scheme.

We now introduce the discrete form of the equations: let Ω be a bounded polygonal domain with dimension $d = 1, 2, 3$ and $\mathcal{T}_\Delta$ a conforming (structured or unstructured) grid on Ω made of either simplex or quad elements. The grid $\mathcal{T}_\Delta$ has n_e elements indicated by $e_r, r = 1, \ldots n_e$ and n_p nodes denoted by $\overrightarrow{x}_k, k = 1, \ldots, n_p$. Let Δ be the maximum diameter of the elements. Consider the dual mesh made of $n_c = n_p$ cells $\tau_k, k = 1, \ldots, n_c$ centered on the nodes $\overrightarrow{x}_k$, and built by connecting the barycenters of the elements to the barycenters of the edges, see Figure 2. Let $\mathbb{I}_k^C = \{k_j, j = 1, \ldots, |\mathbb{I}_k^C|\}$ be the set of the indexes of the cells surrounding cell τ_k, and let $\{\tau_{k_j}, j = 1, \ldots, |\mathbb{I}_k^C|\}$ be the set of cells surrounding τ_k. The common surface between τ_k and τ_{k_j} is indicated by l_k^j. We also indicate by ι the index such that, given the indexes k and j, $\iota : l_{k_j}^\iota = l_k^j$: in other words every interface between the cells τ_k and τ_{k_j} is identified by two different local indexes j; once identified the local index j in τ_k, the other one, in the cell τ_{k_j} is indicated by ι: see Figure 2.

For the sake of clarity, we will adopt in this paper the following convention: the index i will always refer to the fluid species, k to cell related quantities, j to interface related values, r to the elements, and n to the time steps. Let us now introduce the semi-discrete counterparts of λ_i and ϕ_i denoted by $\lambda_{i,\Delta}(t) \in \mathbb{V}^0$, $\phi_{i,\Delta}(t) \in \mathbb{V}^1$, respectively, where $\mathbb{V}^0 = \{\lambda \in L^2(\Omega) : \lambda|_{\tau_k} \in \mathbb{P}^0(\tau_k), \forall k = 1, \ldots, n_c\}$, $\mathbb{V}^1 = \{\phi \in \mathbb{C}^0(\Omega) : \phi|_{e_r} \in \mathbb{Q}^1(e_r), r = 0, \ldots, n_c\}$ in the case of a rectangular grid and $\mathbb{V}^1 = \{\phi \in \mathbb{C}^0(\Omega) : \phi|_{e_r} \in \mathbb{P}^1(e_r), r = 0, \ldots, n_c\}$ on a simplicial mesh. Here $\mathbb{P}^s(\omega)$ denotes the space of polynomials of order at most s on ω, and $\mathbb{Q}^s(\omega)$ is that of the tensor product of polynomials of order at most one. We consider the canonical basis $\{\vartheta_k^0\}$ for $\mathbb{V}^0$ and $\{\vartheta_k^1\}$ for $\mathbb{V}^1$, therefore:

$$\lambda_{i,\Delta}(t, \overrightarrow{X}) = \sum_{k=1}^{n_p} \lambda_{i,k}(t) \vartheta_k^0(\overrightarrow{X}), \quad \phi_{i,\Delta}(t, \overrightarrow{X}) = \sum_{k=0}^{n_c} \phi_{i,k}(t) \vartheta_k^1(\overrightarrow{X}) \tag{5}$$

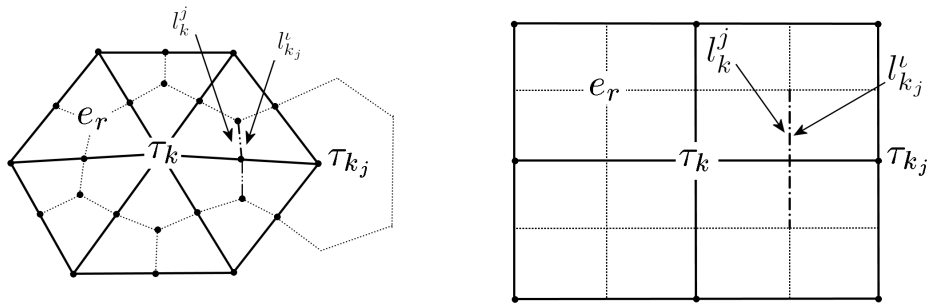

(a) (b)

Figure 2: An example of unstructured (a), and structured (b), two dimensional meshes with the dual meshes (dotted). The $j-th$ neighboring cell of τ_k is τ_{k_j}, the common interface between τ_k and τ_{k_j} is called l_k^j. There is a ι such that the ι-th interface of τ_{k_j} is equal to l_k^j.

where $\lambda_{i,k}$ is the mean volume fraction of the species i in the cell τ_k (we will denote from now on $\lambda_{i,k}$ as the *composition*) and $\phi_{i,k}$ are the values of the discrete level set function at node $\overrightarrow{x}_k$.
We introduce a rather simple coupling between LS and VT equations, by choosing as level set function the piecewise linear interpolator on the dual mesh, i.e. $\phi_{i,\Delta} = \mathbf{I}^1_\Delta \lambda_{i,\Delta}$ where $\mathbf{I}^1_\Delta : \mathbb{V}^0 \to \mathbb{V}^1$ is the linear interpolation operator on the $\mathcal{T}_\Delta$ grid. In other terms we set:

$$\phi_{i,k} = \lambda_{i,k} \quad k = 1, \ldots, n_p, i = 1, \ldots, n_s \tag{6}$$

We advance $\lambda_{i,\Delta}$ by a discrete version of (1), using the information carried by the $\phi_{i,\Delta}$ to build the numerical fluxes, while we reconstruct the level set as a postprocessing. This choice implies an error concerning the representation of the initial conditions as, in general, $\lambda_{i,\Delta} \neq H(\phi_{i,\Delta} - \frac{1}{2})$. This difference can be bounded as we state in the following:

Proposition 2.3 *Let assume that $\lambda \in \mathbb{V}^0$ and has the image in the set $\{1, 0\}$. Consider $\phi = \mathbf{I}^1_\Delta \lambda$. Then:*

$$\int_\Omega \left(\lambda - H\left(\phi - \frac{1}{2} \right) \right) = O(\Delta)$$

Proof: Let $S_b = \{k \in [1, n_c] : \int_{\tau_k} (\lambda - H(\phi - \frac{1}{2})) \neq 0\}$. Since this set is also the set of the cells that are crossed by the boundary of ω its cardinality is $O(\Delta^{1-d})$. Moreover $\int_{\tau_k} (\lambda - H(\phi - \frac{1}{2})) = O(\Delta^d) \forall k \in S_b$, therefore $\int_\Omega (\lambda - H(\phi - \frac{1}{2})) = O(\Delta^{1-d}) O(\Delta^d)$ and we obtain the thesis. ■
Let's now proceed to construct a finite volume method for equation (1). We use

the explicit Euler scheme to discretize the time derivative in (1) and we use (5), obtaining a finite volume scheme for the space discretization, i.e. :

$$\lambda_{i,k}^{n+1} = \left(1 + div_{\Delta,k}^{n}\right) \lambda_{i,k}^{n} - \sum_{j=1}^{|\mathbb{I}_k^C|} F_{i,k}^{n,j} \tag{7}$$

where $\lambda_{i,k}^{n} = \lambda_{i,k}(t^n)$ and $t^0, t^1, \ldots, t^n, t^{n+1}$ is a sequence of time steps with $t^{n+1} = t^n + \Delta t^n$. The quantity $div_{\Delta,k}^{n} = \sum_{j=1}^{|\mathbb{I}_k^C|} \nu_k^{n,j}$ is the discrete dimensionless divergence factor of element τ_k (i.e. $div_{\Delta,k}^{n}$ is the discrete approximation of $\frac{\Delta t^n}{|\tau_k|} \oint_{\partial\tau_k} \overrightarrow{V} \cdot \overrightarrow{n}$) and

$$\nu_k^{n,j} = \frac{\Delta t^n}{|\tau_k|} \int_{l_k^j} \overrightarrow{V} \cdot \overrightarrow{n}$$

is a dimensionless quantity which can be considered as the interface Courant number. The $F_{i,k}^{n,j}(\nu_k^{n,j}, \widehat{\lambda}_{i,k}^{n,j}, \widehat{\lambda}_{i,k_j}^{n,\iota}) = \nu_k^{n,j} \Phi(\widehat{\lambda}_{i,k}^{n,j}, \widehat{\lambda}_{i,k_j}^{n,\iota})$ are the interface fluxes, where $\Phi(\widehat{\lambda}_{i,k}^{n,j}, \widehat{\lambda}_{i,k_j}^{n,\iota})$ is here the upwind function:

$$\Phi(\widehat{\lambda}_{i,k}^{n,j}, \widehat{\lambda}_{i,k_j}^{n,\iota}) = \begin{cases} \widehat{\lambda}_{i,k}^{n,j} \text{ if } \nu_k^{n,j} \geq 0 \\ \widehat{\lambda}_{i,k_j}^{n,\iota} \text{ if } \nu_k^{n,j} < 0 \end{cases} \tag{8}$$

where $\widehat{\lambda}_{i,k}^{n,j}$ is a suitable approximation of the composition $\lambda_{i,\Delta}^{n}|_{\tau_k}$ at the interface l_k^j while $\widehat{\lambda}_{i,k_j}^{n,\iota}$ is another suitable approximation near the interface $l_{k_j}^{\iota} = l_k^j$ from inside τ_{k_j}. For the definition of the interface compositions we have developed

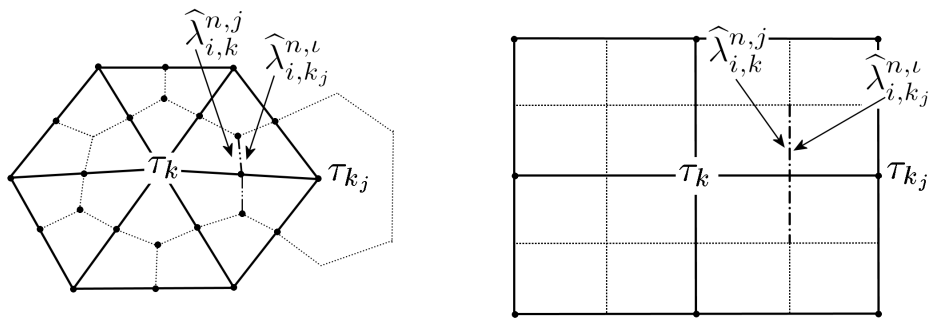

(a) (b)

Figure 3: An example of the boundary compositions $\widehat{\lambda}_{i,k}^{n,j}$ and $\widehat{\lambda}_{i,k_j}^{n,\iota}$ on an unstructured (a), and structured (b) grid. The first is an approximation of the composition from inside τ_k while the other is an approximation from the neighbouring cell τ_{k_j}.

the following scheme. We set for each j, k and i:

$$\widehat{\lambda}_{i,k}^{n,j} = \lambda_{i,k}^{n} + \gamma_{i,k}^{n,j} \Delta\phi_{i,k}^{n,j} \tag{9}$$

where:

$$\Delta\phi_{i,k}^{n,j} = \frac{1}{|l_k^j|}\int_{l_k^j}\phi_{i,\Delta}(t^n) - \frac{1}{|\tau_k|}\int_{\tau_k}\phi_{i,\Delta}(t^n)$$

and $\gamma_{i,k}^{n,j}, i = 1,\dots,n_s$ are the flux limiters defined as the solution of the following constrained minimization problem:

$$\begin{cases} \max\limits_{\gamma_{i,k}^{n,j}\in\mathbb{R}^{n^s}} \sum\limits_{i=1}^{n_s}\gamma_{i,k}^{n,j} \\ \sum\limits_{i=1}^{n_s}\gamma_{i,k}^{n,j}\Delta\phi_{i,k}^{n,j} = 0 \\ 0 \le \gamma_{i,k}^{n,j} \le \gamma_{i,k,max}^{n,j}, i = 1,\dots,n_s \end{cases} \tag{10}$$

where:

$$\begin{cases} \gamma_{i,k,max}^{n,j} = \min\left(1, \dfrac{(1+div_{\Delta,k}^n) - \nu_k^{n,j}|\mathbb{J}_k|}{\nu_k^{n,j}|\mathbb{J}_k|\Delta\phi_{i,k}^{n,j}}\lambda_{i,k}^n, \dfrac{1-\lambda_{i,k}^n}{\Delta\phi_{i,k}^{n,j}}\right) \text{ if } \Delta\phi_{i,k}^{n,j} > 0 \\ \gamma_{i,k,max}^{n,j} = \min\left(1, -\dfrac{\lambda_{i,k}^n}{\Delta\phi_{i,k}^{n,j}}\right) \text{ if } \Delta\phi_{i,k}^{n,j} < 0 \\ \gamma_{i,k,max}^{n,j} = 1 \text{ if } \Delta\phi_{i,k}^{n,j} = 0 \end{cases} \tag{11}$$

and $\mathbb{J}_k$ is the set of the indices of the outflow faces l_k^j of the k-th cell i.e:

$$\mathbb{J}_k = \left\{ j \in 1,\dots|\mathbb{I}_j^C| : \nu_k^{n,j} \ge 0 \right\}$$

As we have dropped the usual definition of the distance function we need to define a proper reinizialization algorithm for the composition $\lambda_{i,k}^n$ (the level set is then updated using (6)):

Algorithm 1 *If there is an index $\bar{i}$ such that:*

$$\lambda_{\bar{i},k}^n > \frac{1}{2} \text{ and } \lambda_{\bar{i},k_j}^n > \frac{1}{2} \quad \forall j \in \mathbb{I}_k^C \tag{12}$$

then we set $\lambda_{\bar{i},k}^n = 1$ and $\lambda_{i,k}^n = 0$ with $i = 1,\dots,n_s, i \ne \bar{i}$. Otherwise we mantain the nodal value $\lambda_{i,k}^n$.

In fact if equation (12) is satisfied, from (6) we have that $\tau_k \in \omega_i$ and therefore we may set $\lambda_{\bar{i},k}^n = 1$. This algorithm doesn't modify the LS function in all the elements where $\phi_{i,\Delta}^n$ equals $\frac{1}{2}$: in other words, the interfaces are not modified by this algorithm. Since the evolution of the interfaces is independent of the set function (see [17], [22]) this algorithm doesn't introduce any error from the LS point of view. Having concluded the definition of our method we devote the next section to its analysis.

3 Analysis

Proposition 3.1 *Problem (10) has at least one solution.*

Proof:
We have to prove that the feasible region is nonempty. Indeed $\gamma_{i,k}^{n,j} = 0$ satisfies all the constraints and then we obtain the result. ■

Proposition 3.2 *The method defined by (9), (10) (11) is positive, i.e.* $\lambda_{i,k}^{n+1} \geq 0$, $\forall i, \forall k$.

Proof:
For $n = 0$ the initial data satisfy the requirement and we proceed by induction, we suppose $\lambda_{i,k}^{n} \geq 0$. From (11) we have:

$$\gamma_{i,k}^{n,j} \leq \frac{(1 + div_{\Delta,k}^{n}) - \nu_k^{n,j}|\mathbb{J}_k|}{\nu_k^{n,j}|\mathbb{J}_k|\Delta\phi_{i,k}^{n,j}}\lambda_{i,k}^{n} \text{ if } \Delta\phi_{i,k}^{n,j} > 0$$

and after a few manipulations we get the following bound for the fluxes:

$$\begin{cases} F_{i,k}^{n,j} \leq 0 \text{ if } \nu_k^{n,j} < 0 \\ F_{i,k}^{n,j} \leq \dfrac{1 + div_{\Delta,k}^{n}}{|\mathbb{J}_k|}\lambda_{i,k}^{n} \text{ if } \nu_k^{n,j} \geq 0 \end{cases}$$

Therefore we can also bound the sum of the interface fluxes:

$$\sum_{j=1}^{|\mathbb{I}_k^C|} F_{i,k}^{n,j} \leq \sum_{j \in \mathbb{J}_k} \frac{1 + div_{\Delta,k}^{n}}{|\mathbb{J}_k|}\lambda_{i,k}^{n} \leq 1 + div_{\Delta,k}^{n}\lambda_{i,k}^{n}$$

Using (7) and using the fact that $\lambda_{i,k}^{n} \geq 0$ is positive we obtain the proof. ■

Proposition 3.3 *At every time step the sum of partial volumes on every cell equals one, that is:*

$$\sum_{i=1}^{n_s} \lambda_{i,k}^{n} = 1 \quad \forall n, \forall k = 1, \ldots, n_c \tag{13}$$

Analogously, the sum of the level set functions is everywhere equal to one:

$$\sum_{i=1}^{n_s} \phi_{i,\Delta}^{n} = 1 \quad \forall n$$

Proof:
Let's use the induction principle. At $n = 0$, condition (13) is satisfied by construction. Let us assume that the condition is satisfied at time t^n. We have:

$$\sum_{i=1}^{n_s} \lambda_{i,k}^{n+1} = \sum_{i=1}^{n_s} \left[\left(1 + div_{\Delta,k}^n\right) \lambda_{i,k}^n - \sum_{j=1}^{|\mathbb{I}_k^C|} F_{i,k}^{n,j} \right] =$$
$$\left(1 + div_{\Delta,k}^n\right) - \sum_{i=1}^{n_s} \sum_{j=1}^{|\mathbb{I}_k^C|} \nu_k^{n,j} \Phi(\widehat{\lambda}_{i,k}^{n,j}, \widehat{\lambda}_{i,k_j}^{n,\iota}) = 1$$

by which (13) follows. Since $\phi_{i,\Delta}^n = \sum_{k=1}^{n_c} \lambda_{i,k}^n \vartheta_k^1$ we get:

$$\sum_{i=1}^{n_s} \phi_{i,\Delta}^n = \sum_{i=1}^{n_s} \sum_{k=1}^{n_c} \lambda_{i,k}^n \vartheta_k^1 = \sum_{k=1}^{n_c} \vartheta_k^1 = 1$$

■

We now examine the consistence of the scheme.

Proposition 3.4 *If the solution is smooth, the method defined by (7) is consistent.*

Proof:
We will show that, if the solution is regular enough, for $\Delta \to 0$, the modified solution of our scheme equals almost everywhere the modified solution of the Godunov scheme and that $\lim_{\Delta x \to 0} div_{\Delta,k}^n \to \Delta t^n (\overrightarrow{\nabla} \cdot \overrightarrow{V})$. The Godunov method is defined by:

$$g_{i,k}^{n,j} = \Phi(\lambda_{i,k}^n, \lambda_{i,k_j}^n) = \begin{cases} \lambda_{i,k}^n \text{ if } \nu_k^{n,j} \geq 0 \\ \lambda_{i,k_j}^n \text{ if } \nu_k^{n,j} < 0 \end{cases} \tag{14}$$

And the corresponding Godunov's numerical flux $G_{i,k}^{n,j}(\nu_k^{n,j}, \lambda_{i,k}^n, \lambda_{i,k_j}^n) = \nu_k^{n,j} g_{i,k}^{n,j}$ satisfies the following consistency properties:

$$\begin{cases} G_{i,k}^{n,j}(\nu_k^{n,j}, \lambda_{i,k}^n, \lambda_{i,k_j}^n) = -G_{i,k}^{n,j}(-\nu_k^{n,j}, \lambda_{i,k}^n, \lambda_{i,k_j}^n) \\ G_{i,k}^{n,j}(\nu_k^{n,j}, \lambda_{i,k}^n, \lambda_{i,k}^n) = \dfrac{\Delta t^n}{|\tau_k|} \displaystyle\int_{l_k^j} \lambda_{i,k}^n \overrightarrow{V} \cdot \overrightarrow{n} \end{cases} \tag{15}$$

It's worth noting that our scheme, defined by (8) and (11), and the Godunov method differ only in the definition of the interface states. In fact, our scheme corrects the cell mean value with the term:

$$\gamma_{i,k}^{n,j} \Delta \phi_{i,k}^{n,j} \tag{16}$$

Therefore, if this term vanishes for $\Delta \to 0$, we get the first part of the proof. Let $u_i(t, \overrightarrow{X})$ be the modified solution such that:

$$u_i(t^n, \overrightarrow{x}_k) = \lambda_{i,k}^n; \quad \forall n, \quad \forall i = 1, \ldots, n_s, \quad k = 1, \ldots, n_c \tag{17}$$

and suppose the modified solution is regular enough so that the following relation holds:

$$u_i(\overrightarrow{X}) = u_i(\overrightarrow{Y}) + \overrightarrow{\nabla} u_i \cdot (\overrightarrow{X} - \overrightarrow{Y}) + O(|\overrightarrow{X} - \overrightarrow{Y}|^2)$$

Since $\phi_{i,\Delta}$ is continuous, from (6) we have:

$$\Delta\phi_{i,k}^{n,j} = \frac{1}{|l_k^j|}\int_{l_k^j} \phi_{i,\Delta}(t^n) - \frac{1}{|\tau_k|}\int_{\tau_k} \phi_{i,\Delta}(t^n) =$$
$$\frac{1}{|l_k^j|}\int_{l_k^j} u_i(\overrightarrow{X}_k) + O(\Delta) - \frac{1}{|\tau_k|}\int_{\tau_k} u_i(\overrightarrow{X}_k) + O(\Delta) = O(\Delta)$$

Since $\gamma_{i,k}^{n,j}$ is bounded, we obtain the first part of the proof. Let's now consider the second part. We have:

$$div_{\Delta,k}^n = \frac{\Delta t^n}{|\tau_k|}\sum_{j=1}^{|\mathbb{I}_k^C|}\int_{l_k^j} \overrightarrow{V}\cdot\overrightarrow{n} = \frac{\Delta t^n}{|\tau_k|}\oint_{\partial\tau_k} \overrightarrow{V}\cdot\overrightarrow{n} = \frac{\Delta t^n}{|\tau_k|}\int_{\tau_k} \overrightarrow{\nabla}\cdot\overrightarrow{V} \tag{18}$$

and as $\Delta \to 0$ we get the desired result. ■

Let's now move to the properties of the level set. Relation (6) allows us to get a LS representation starting from the cell partial volumes. We show that this method has an interesting property that makes it most suitable for immiscible multi-fluid simulations. First we define the discrete subdomain associated to the i-th species as:

$$\widetilde{\omega}_{i,\Delta}(t) = \left\{\overrightarrow{P} \in \Omega : \phi_{i,\Delta}(t, \overrightarrow{P}) > \frac{1}{2}\right\}$$

Then we can prove the following statement

Proposition 3.5 *Every discrete subdomain does not overlap with the others, i.e:*

$$\widetilde{\omega}_{i,\Delta}(t) \cap \widetilde{\omega}_{j,\Delta}(t) = \emptyset \quad \forall i = 1,\ldots,n_s, \quad \forall j = 1,\ldots,n_s, j \neq i \quad \forall t > 0$$

and given a subregion $\widetilde{\Omega} \subset \Omega$ containing only two species identified by the indices i_1, i_2, we have:

$$\overline{\widetilde{\omega}}_{i_1,\Delta} \cup \overline{\widetilde{\omega}}_{i_2,\Delta} = \overline{\widetilde{\Omega}}$$

Proof:
If $\overrightarrow{X} \in \omega_i(t)$ then $\phi_{i,\Delta}(t, \overrightarrow{X}) > \frac{1}{2}$ and from proposition (3.3) we get:

$$\sum_{j=1, j\neq i}^{n_s} \phi_{i,\Delta}(t, \overrightarrow{X}) < \frac{1}{2}$$

Since the level set functions are piecewise linear interpolations of a positive function (the volume fractions $\lambda_{i,\Delta}$) we get $\phi_{j,\Delta}(t, \overrightarrow{X}) < \frac{1}{2} \quad \forall j \neq i$ i.e. $\overrightarrow{X} \notin \omega_j(t) \quad \forall j \neq i$. In the special case of a subregion $\widetilde{\Omega}$ which contains only two

species, we get from the general case that there is no overlap between the two subdomains $\widetilde{\omega}_{i_1,\Delta}$, $\widetilde{\omega}_{i_2,\Delta}$. We have only to prove that:

$$\overrightarrow{X} \in \widetilde{\omega}_{i_1,\Delta} \text{ or } \overrightarrow{X} \in \widetilde{\omega}_{i_2,\Delta} \text{ or } \overrightarrow{X} \in \overline{\widetilde{\omega}}_{i_1,\Delta} \cap \overline{\widetilde{\omega}}_{i_2,\Delta} \quad \forall \overrightarrow{X} \in \widetilde{\Omega}$$

We consider three cases:

$$\begin{cases} \phi_{i_1,\Delta}(t,\overrightarrow{X}) > \frac{1}{2}, \text{ then } \overrightarrow{X} \in \widetilde{\omega}_{i_1,\Delta} \\ \phi_{i_1,\Delta}(t,\overrightarrow{X}) < \frac{1}{2}, \text{ so } \overrightarrow{X} \in \widetilde{\omega}_{i_2,\Delta}, \text{ in fact: } \phi_{i_2,\Delta}(t,\overrightarrow{X}) = 1 - \phi_{i_1,\Delta}(t,\overrightarrow{X}) \\ \phi_{i_1,\Delta}(t,\overrightarrow{X}) = \frac{1}{2}, \text{ consequently, point } \overrightarrow{X} \in \overline{\widetilde{\omega}}_{i_1,\Delta} \cap \overline{\widetilde{\omega}}_{i_2,\Delta} \end{cases} \tag{19}$$

Therefore we get the thesis. ■

4 The analysis of the one-dimensional case

In one dimension a more detailed analysis is possible. Let $\mathcal{T}_\Delta$ be a uniformily Δx-spaced 1D mesh (see Figure 4) with elements $e_0, \ldots, e_{r-1}, e_r, e_{r+1}, \ldots, e_{n_e}$ and consider its dual mesh endowed with an ordered sequence of cells $\tau_0, \ldots, \tau_{k-1}, \tau_k, \tau_{k+1}, \ldots, \tau_{n_c}$. For the sake of simplicity let V be a constant, positive velocity field (i.e. we are treating a null divergence case), and $\nu^n = \frac{\Delta t^n}{\Delta x} V$ the Courant number. Notice that, in this case, all the Courant numbers are equivalent to ν^n. Besides, every cell is associated to a mean composition $\lambda^n_{i,0}, \ldots, \lambda^n_{i,k-1}, \lambda^n_{i,k}, \lambda^n_{i,k+1}, \ldots, \lambda^n_{i,n_c}$ and has two boundary sub-cells $\widehat{\lambda}^{n,j}_{i,k}$ with $j = 1, 2$. Using a

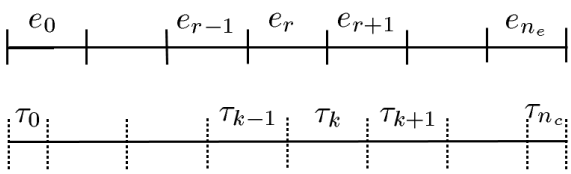

Figure 4: The one dimensional mesh. In the upper part are depicted the mesh and the elements e_r while in the lower part the dual mesh is shown along with its cells τ_k.

more explicit notation in 1D we can define the upwind subcell as $\widehat{\lambda}^{n,+}_{i,k}$ and the downwind subcell as $\widehat{\lambda}^{n,-}_{i,k}$, in the same manner we can define also $\Delta\phi^{n,+}_{i,k}$ and $\Delta\phi^{n,-}_{i,k}$. Thus we have:

$$\Delta\phi^{n,+}_{i,k} = -\Delta\phi^{n,-}_{i,k} = \frac{\lambda^n_{i,k+1} - \lambda^n_{i,k-1}}{2} \tag{20}$$

and method (7) takes the form:

$$\begin{cases} \lambda^{n+1}_{i,k} = \lambda^n_{i,k} - \nu(\widehat{\lambda}^{n,+}_{i,k} - \widehat{\lambda}^{n,+}_{i,k-1}) \\ \widehat{\lambda}^{n,+}_{i,k} = \lambda^n_{i,k} + \gamma^{n,+}_{i,k} \dfrac{\lambda^n_{i,k+1} - \lambda^n_{i,k-1}}{2} \end{cases} \tag{21}$$

In the one dimensional case it is possible, using the modified equation technique, to carry out a convergence analysis. We need first the following:

Proposition 4.1 *If the solution of the modified equation (defined in (17)) is regular enough, the limiter $\gamma_{i,k}^{n,j}$ defined by (10) tends to one as $\Delta \to 0$.*

Proof:
Substituting the estimate (3) in (11) we get $\gamma_{i,k,max}^{n,j} \to 1$. ■

Proposition 4.2 *The method defined by (20) and (21) is second order accurate in space and first order accurate in time.*

Proof:
We use a standard modified equation argument, using (17) we get:

$$\begin{aligned}
\lambda_{i,k+1}^{n} &= u(t^n, x_k) + \frac{\partial}{\partial x} u(t^n, x_k)\Delta x + \frac{\partial^2}{\partial x^2} u(t^n, x_k)\Delta x^2 + O(\Delta x^3) \\
\lambda_{i,k-1}^{n} &= u(t^n, x_k) - \frac{\partial}{\partial x} u(t^n, x_k)\Delta x + \frac{\partial^2}{\partial x^2} u(t^n, x_k)\Delta x^2 + O(\Delta x^3) \\
\lambda_{i,k}^{n+1} &= u(t^n, x_k) + \frac{\partial}{\partial t} u(t^n, x_k)\Delta t + \frac{\partial^2}{\partial t^2} u(t^n, x_k)\Delta t^2 + O(\Delta t^3)
\end{aligned}$$

Substituting in the second of (21) we obtain:

$$\begin{aligned}
\widehat{\lambda}_{i,k}^{n,+} &= u(t^n, x_k) + \frac{\partial}{\partial x} u(t^n, x_k)\Delta x + O(\Delta x^3) \\
\widehat{\lambda}_{i,k-1}^{n,+} &= u(t^n, x_{k-1}) + \frac{\partial}{\partial x} u(t^n, x_{k-1})\Delta x + O(\Delta x^3)
\end{aligned}$$

and combining them with the first of (21) we get:

$$\Delta t^n \frac{\partial}{\partial t} u(t^n, x_k) + O((\Delta t^n)^2) = -\frac{\Delta t^n}{\Delta x} V \left(u(t^n, x_k)\Delta x - u(t^n, x_{k-1})\Delta x + \frac{\partial}{\partial x} u(t^n, x_k)\Delta x^2 - \frac{\partial}{\partial x} u(t^n, x_{k-1})\Delta x^2 + O(\Delta x^3) \right)$$

Finally, dividing by Δt^n we obtain:

$$\frac{\partial}{\partial t} u(t^n, x_k) + V \frac{\partial}{\partial x} u(t^n, x_k) = O(\Delta t^n) + O(\Delta x^2)$$

and the proof follows. ■

5 Results

In this section we introduce some numerical results: the first one is the convergence result in one dimension. In this case, in order to accomodate the boundary conditions, we have introduced a slight modification to the algorithm. In the

description of this method we have, so far, neglected the boundary conditions since we wanted to focus on the properties of the method which are not dependent from them. We consider a test case with a constant transport speed i.e. $v = 1$ and the domain Ω is the interval $[0, 1]$. The initial conditions are $\lambda^0_{1,k} = 1, \lambda^0_{2,k} = 0 \quad \forall k$, while $\lambda^b_1(t) = 0, \lambda^b_2(t) = 1 \quad \forall t \in [0, T]$ are the boundary conditions on the left (inflow) side. The problem

$$\frac{\partial \lambda_i}{\partial t} + v \frac{\partial \lambda_i}{\partial x} = 0$$

has the following analytical solution:

$$\lambda_1(t, x) = H(x - vt), \quad \lambda_2(t, x) = 1 - H(x - vt)$$

and it is possible to compute the L^1 error on $(0, T) \times (0, 1)$ defined as:

$$E_{L^1} = \sum_{i=1}^{n_s} \int_0^T \int_a^b |\lambda_i(t, x) - \lambda_{i,\Delta}(t, x)|$$

In Figure 5 we show the L^1 error of the proposed method compared with a high resolution Discontinuous Galerkin (DG) method with a MinMod Limiter, see [8] and with the Godunov (G) method. Our method compares favorably with the

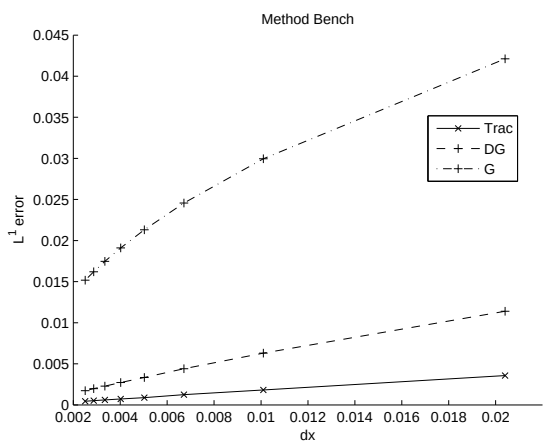

Figure 5: One dimensional convergence of the proposed method (Trac) compared with a Discontinuous Galerkin (DG) method and with the Godunov (G) method.

DG method though the regularity of the solution limits the convergence rate. In fact, in this case, both our method and the DG method are only first order accurate.

Let's now consider some classical examples in two dimensions; in Figure 6a we outline some results obtained with a rotational field, $\overrightarrow{V}(\overrightarrow{X}) = [-X_2 - 1, X_1 - 1]$

where X_1, X_2 are the cartesian components of $\overrightarrow{X}$. A square is filled with a fluid tagged as A, the remaining space is filled with a fluid tagged as B; the square lower left corner coordinates are $[0.8, 0.2]$ and the upper right corner coordinates are $[1.2, 0.6]$. If we compare with the comprehensive benchmark

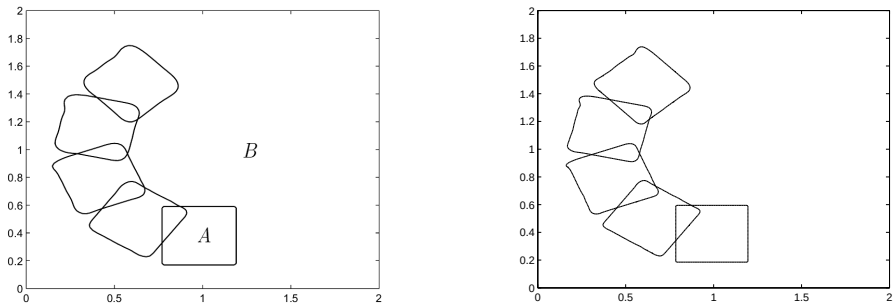

(a) (b)

Figure 6: Tracking of a square with (a) 10000 degrees of freedom and $cfl = \frac{1}{10}$ and (b) 40000 degrees of freedom and $cfl = \frac{1}{10}$.

analysis performed in [10] we see that our results are intermediate nevertheless our method has the possibility to track a large number of fluids as we show in Figure 7. Here we consider the same case but with three fluids: the first, tagged as A, fills the inner square, the outer is filled with fluid B and the remaining space in the domain is filled with fluid C, see Figure 7a. The inner square lower left corner and upper right coordinates are respectively $[0.9, 0.3]$, $[1.1, 0.5]$ while the outer square corners coordinates are $[0.8, 0.2]$, $[1.2, 0.6]$. As we can see from Figure 7 the tracking performances are independent from the number of the species being tracked. In Figure 8 we track three non-nested fluids showing the coherence between the three tracked interfaces: the small rectangle filled with fluid C has the following corner coordinates $[0.75, 1]$, $[1.25, 1.45]$. The fluid B fills a more complex region that is the complementary part of the rectangle C in a rectangle with corner coordinates $[0.5, 0.45]$, $[1.5, 1.45]$. The remaining part of the computational domain is filled with the fluid A. The methodology proposed here has been also implemented in three dimensions. We study a rising bubble numerical test case that can be considered an extension to three fluids of the two fluid cases examined, for instance, in [19], [25], [23], [28]. We have considered a unit cube filled with three species, the first one lies on the bottom of the cube and form a 0.2-thick layer. The second one form a 0.6-thick layer, while the third one is 0.2-thick. A small perturbation is applied to the interface between the first and second layer in order to trigger a gravitational instability. In Figure 9 the evolution of the three layers is shown. A primary bubble is formed, during the ascension it pierces the two surrounding layers and finally it detaches from the bottom. Also four secondary bubbles are crated on the

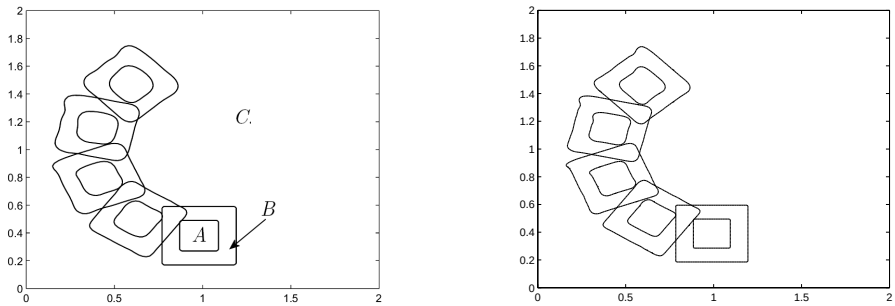

(a) (b)

Figure 7: Tracking of two nested squares with (a) 10000 degrees of freedom and $cfl = \frac{1}{10}$ and (b) 40000 degrees of freedom and $cfl = \frac{1}{10}$. In this case three species are involved: the inner square is filled with the species A, the outer with species B and the rest of the domain with species C.

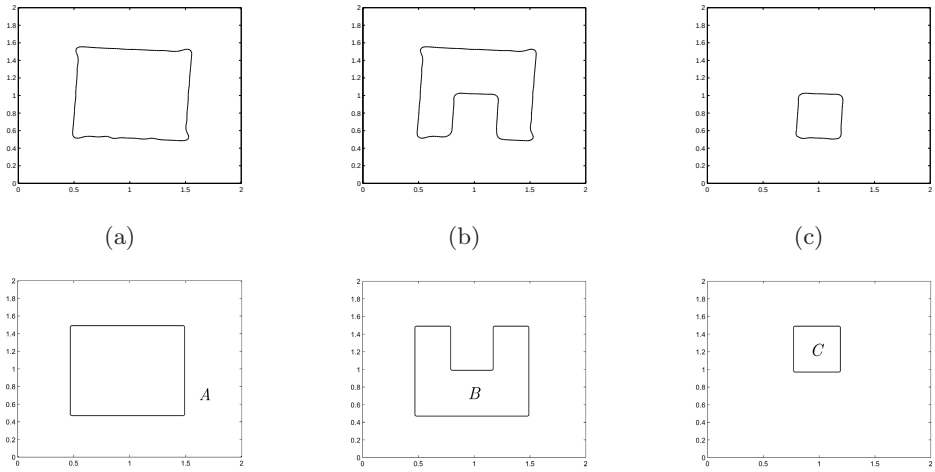

(a) (b) (c)

(d) (e) (f)

Figure 8: Multi-fluid tracking using 10000 degrees of freedom and $cfl = \frac{1}{5}$. (a),(b),(c) are the computed interfaces after half a turn and (d),(e),(f) are the initial configurations.

boundary. In this simulation multiple topology changes are handled in a natural way and a coherent representation of the separating interfaces between the layers is shown.

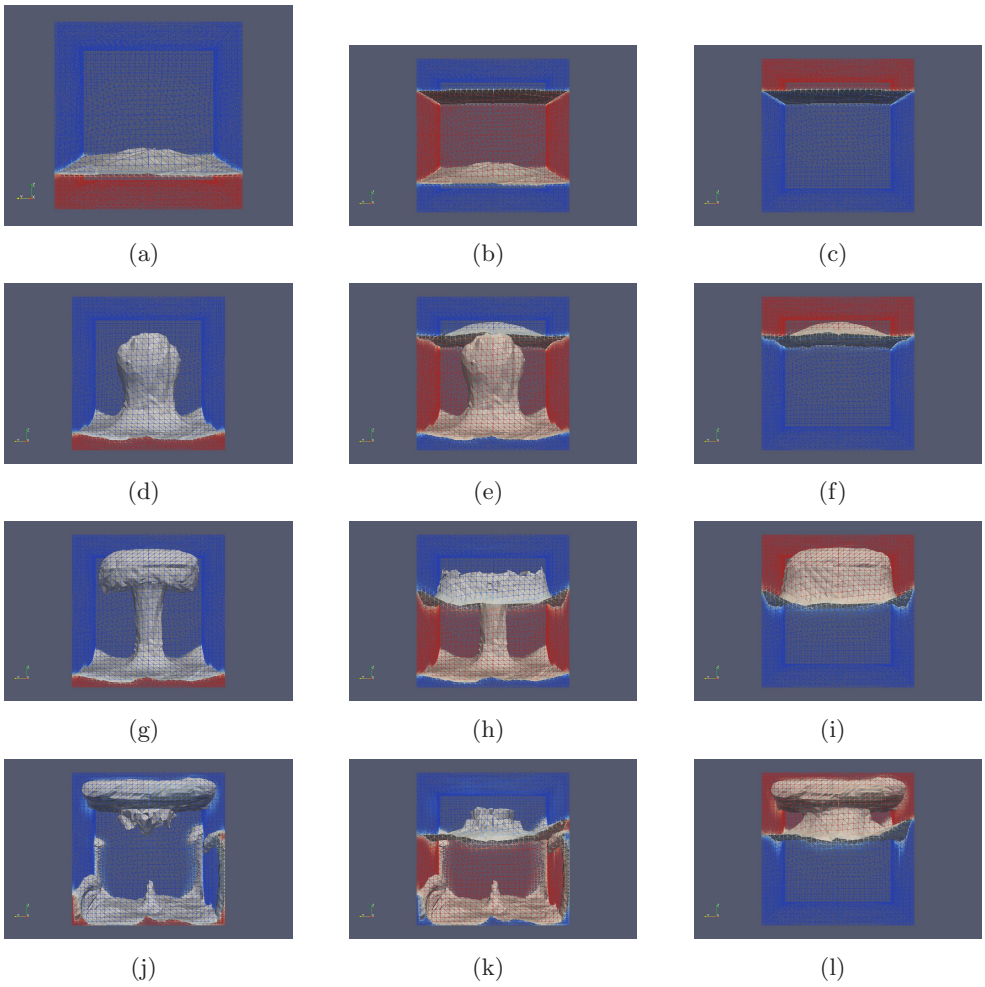

Figure 9: The evolution of a rising bubble. It pierces two layers yielding the formation of a primary bubble and four secondary bubbles on the boundary.

6 Conclusions

We have devised a coupled level set volume tracking method, the method has been implemented in one, two and three dimensions. It is computationally efficient and able to perform on general unstructured grids. It is currently used in geophysical simulations where the velocity field is computed by solving a Stokes problem [21] and has demonstrated its flexibility in treating complex simulations. Because of its local structure, it is easily parallelizable. In forthcoming works we'll show more details about applications to the multi-fluid geological simulations and we investigate some higher performance implementation of our code.

Acknowledgements The authors wish to acknowledge the support of the

Italian MIUR (grant PRIN 2007). They also wish to thank G.Scrofani and P.Ruffo for having supported such interesting research project.

References

[1] A. Anderson, X. Zheng, V. Cristini. Adaptive unstructured volume remeshing - 1: The method. J. Comput. Phys. 208, 616-625. 2005.

[2] A. Anderson, J. Lowengrub, X. Zheng, V. Cristini. Adaptive unstructured volume remeshing - 2: Applications to two-and three-dimensional level-set simulations of multiphase flow. J. Comput. Phys. 208, 626-650. 2005.

[3] E. Aulisa, S. Manservisi, R. Scardovelli. A surface marker algorithm coupled to an area-preserving marker redistribution method for three-dimensional interface tracking. J. Comput. Phys. 197, 555-584. 2004.

[4] E. Aulisa, S. Manservisi, R. Scardovelli. A mixed markers and volume-of-fluid method for the reconstruction and advection of interfaces in two-phases and free-boundary flows. J. Comput. Phys. 188, 611-639. 2003.

[5] P. Batten, C. Lambert, D.M. Causon. Positively conservative high resolution convection scheme for unstructured elements. Int. J. Numer. Methods Eng. 39, 1821-1838. 1996.

[6] T. Brochu, R. Bridson. Fluid Animation with Explicit Surface Meshes. ACM SIGGRAPH Symposium. 2006.

[7] A. Caboussat. Numerical Simulation of Two-Phase Free Surface Flows. Arch. Comput. Meth. Eng. 12, 2, 165-224. 2005.

[8] B. Cockburn, C.W. Shu. TVB Runge Kutta local projection discontinuous Galerkin finite element method for conservation laws 2: general framework. Mathematics of Computing. 52, 411-435. 1989.

[9] R. M. Darlington, T. L. McAbee, G. Rodrigue. A study of ALE simulations of Rayleigh-Taylor instability. Comput. Phys. Commun. 135 58-73. 2001.

[10] D. A. Di Pietro, S. Loforte, N. Parolini. Mass preserving finite element implementations of the level set method. Appl. Numer. Math. 56, 1179-1195. 2006.

[11] Douglas, B. Kothe. Perspective on Eulerian finite volume methods for incompressible interfacial flows. Kuhlmann and H Rath, 267-331. 1999.

[12] J. Glimm, J. W. Grove, X. L. LI, K. Shyue, Y. Zeng, Q. Zhang. Three-dimensional front tracking. SISC. 19, 703-727. 1998.

[13] R. J. LeVeque. Numerical Methods for Conservation Laws. Birkhauser. 1999.

[14] P. D. Minev, T. Chen, K. Nandakumar. A finite element technique for multigrid incompressible flow using eulerin grids. J. Comput. Phys. 187 255-273. 2003.

[15] K. Ohmori, N. Saito. Flux-free Finite Element Method with Lagrange Multipliers for Two-fluid Flows. SISC. 32, 147-173. 2004.

[16] E. Onate, S.R. Idelsohn, F. Del Pin, R. Aubry. The particle finite element method. An overview. Int. J. Comput. Methods. 1, 2, 267-307. 2004.

[17] S. Osher, R. P. Fedkiw. Level Set Methods and Dynamic Implicit Surfaces. Springer 2003.

[18] P. Pedragal. Introduction to optimization. Springer 2004.

[19] S. P. van der Pijl, A Segal, C. Vuik, P. Wesseling. A mass-conserving level-set method for modelling of multi-phase flows. Int. J. Numer. Methods Fluids. 47, 339-361. 2005.

[20] S. Popinet, S. Zaleski. A front-tracking algorithm for accurate representation of surface tension. International Journal for Numerical Methods in Fluids. 30, 775 - 793. 1999.

[21] A. Scotti, A. Villa. Predictive numerical models of basin evolution and petroleum generation. To appear in: Communications to SIMAI Congress 2008.

[22] A. Sethian. Level Set Methods and Fast Marching Methods. Cambridge University Press. 1999.

[23] S. Shin, D. Juric. Modeling three-dimensional multiphase flow using a level contour reconstruction method for front tracking without connectivity. J. Comput. Phys. 180, 427-470. 2002.

[24] A. Smolianski. Finite-Element/level-Set/Operator-Splitting (FELSOS) approach for computing two-fluid unsteady flows with free moving interfaces. Int. J. Numer. Methods Fluids. 24, 231-269. 2004.

[25] M. Sussman, E. Fatemi, P. Smereka, S. Osher. An improved level set method for incompressible two-phase flows. Comp. Fluids. 27, 663-680. 1998.

[26] M. Sussman, E. G. Puckett. A coupled level set and volume-of-fluid method for computing 3D and axisymmetric incompressible two-phase flows. J. Comput. Phys. 162, 301-337. 2000.

[27] D. J. Torres, J. U. Brackbill. The Point-Set Method: Front-Tracking without Connectivity. J. Comput. Phys. 165, 620-644. 2000.

[28] G. Tryggvason, B. Brunner, A.Esmaeeli, D.Juric, N. Al-Rawahi, W.Tauber, J.Han, S. Nas, Y.-J Jant. A front-tracking method for the computations of multiphase flow. J. Comput. Phys. 169, 708-759. 2001.

MOX Technical Reports, last issues

Dipartimento di Matematica "F. Brioschi",
Politecnico di Milano, Via Bonardi 9 - 20133 Milano (Italy)

11/2009 L. Formaggia, A. Villa:
Implicit tracking for multi-fluid simulations

10/2009 P. Zunino:
Numerical approximation of incompressible flows with net flux defective boundary conditions by means of penalty techniques

09/2009 E. Agostoni, S. Salsa, M. Perego, A. Veneziani:
Mathematical and Numerical Modeling of Focal Cerebral Ischemia

08/2009 P.F.Antonietti, P.Houston:
An hr-adaptive discontinuous Galerkin method for advection-diffusion problems

07/2009 M. Perego, A. Veneziani:
An efficient generalization of the Rust-Larsen method for solving electrophysiology membrane equations

06/2009 L. Formaggia, A. Veneziani, C. Vergara:
Numerical solution of flow rate boundary for incompressible fluid in deformable domains

05/2009 F. Ieva, A.M. Paganoni:
A case study on treatment times in patients with ST-Segment Elevation Myocardial Infarction

04/2009 C. Canuto, P. Gervasio, A. Quarteroni:
Finite-Element Preconditioning of G-NI Spectral Methods

03/2009 M. D'Elia, L. Dedé, A. Quarteroni:
Reduced Basis Method for Parametrized Differential Algebraic Equations

02/2009 L. Bonaventura, C. Biotto, A. Decoene, L. Mari, E. Miglio:
A couple ecological-hydrodynamic model for the spatial distribution of sessile aquatic species in thermally forced basins